Drop Breakup in Turbulent Stirred-Tank Contactors

Part I: Effect of Dispersed-Phase Viscosity

The extent to which dispersed-phase viscosity influences equilibrium mean drop size and drop size distribution at constant interfacial tension is determined for dilute suspensions by dispersing silicone oils of various viscosity grades in water. A mechanistic model for mean drop size is developed which predicts the moderate-viscosity data and whose parameters correlate the high-viscosity results. Trends in the mean size data coincide with those for the drop size distribution, which broadens considerably as viscosity increases and suggests a dependency on breakage mechanism.

R. V. Calabrese
Department of Chemical and Nuclear
Engineering
University of Maryland
College Park, MD 20742

T. P. K. Chang and P. T. Dang
Department of Chemistry and Chemical
Engineering
Stevens Institute of Technology
Hoboken, NJ 07030

SCOPE

Drops are stabilized in dilute agitated liquid-liquid systems by surface and dispersed-phase viscous forces and are broken up by forces associated with the continuous-phase turbulence. Most studies have been limited to surface force stabilized dispersions, so the extent to which dispersed-phase viscosity influences mean drop size and drop size distribution is not well understood.

For inviscid dispersed phases, equilibrium mean drop sizes produced by turbulent stirred-tank contacting processes are correlated by the well-known Weber number theory. This semiempirical theory, as applied to dilute suspensions, has been extended via mechanistic arguments to account for the effect of dispersed-phase viscosity. A viscosity group, N_{Vi}, is introduced which accounts for the importance of dispersed-phase viscosity relative to interfacial tension.

Numerous experiments were conducted in four, baffled cylindrical tanks of standard geometry, equipped with six-blade Rushton turbines, by photographically examining dilute suspensions of silicone oils in water. Five grades of oil, ranging in viscosity from about 0.1 to 10 Pa · s and exhibiting the same interfacial tension with water ([0.0378 N/m), were employed. The range of variables studied includes $13,000 < Re < 101,000$, $44 < We < 1,137$, and $0.065 < \epsilon < 0.50$ m^2/s^3. The objectives of the experimental program were to examine the extent to which dispersed-phase viscosity influences equilibrium mean drop size and drop size distribution at constant interfacial tension, and to determine the relevance of the predicted correlating parameters and the range of applicability of the semiempirical theory.

Results are compared to the data of Chen and Middleman (1967) for inviscid dispersed phases and the limited data of Arai et al. (1977) for viscous drops. Trends in the data are interpreted in light of the relevant correlating variables, the functional form of the drop size distribution, and the mechanism of drop breakup.

CONCLUSIONS AND SIGNIFICANCE

The experimental data have been analyzed and compared to the derived correlations and to literature data for inviscid dispered phases. The following conclusions apply to the range of variables studied.

1. At constant conditions of agitation, the equilibrium drop size distribution broadens considerably as dispersed-phase viscosity, μ_d, increases. The size of the smallest drops decreases, while their number increases. The size of the largest drops increases, while their number decreases. Moderate viscosity ($\mu'_d = 0.1$ and 0.5 Pa · s) dispersed phases are normally distributed in number, while high-viscosity drops ($\mu'_d = 5$ and 10 Pa · s) exhibit a log-normal number distribution. The functional form of the distribution for the intermediate oil ($\mu'_d = 1$ Pa · s) cannot be characterized. The Sauter mean diameter for the high-viscosity oils is determined by the largest drops.

2. Given the scatter in the data, the ratio of Sauter mean diameter, D_{32}, to maximum stable drop size, D_{max}, is approximately the same for both inviscid and viscous dispersed phases. However, D_{32}/D_{max} does decrease, to some extent, as μ_d increases.

3. The derived correlation (Eq. 18 and Figure 5) predicts the moderate-viscosity data fairly well but fails at higher dispersed-phase viscosities. However, the parameters of the model, D_{32}/D_o and N_{Vi}, are the correct correlating variables for the high-viscosity oils. A transition occurs at intermediate viscosity, indicating that the assumption of dynamic similarity inherent in the model may not be valid over the entire μ_d range. The limited data of Arai et al. (1977) show some of the same trends as the data of this study.

4. It appears that interfacial tension ($\sigma = 0.0378$ N/m) still contributes to drop stability for the high-viscosity oils since the correlation that applies to the limit of negligible surface resistance cannot completely describe these data.

5. Sauter mean diameter is well correlated by μ_d and either tank Reynolds number or tip speed. However, the dependency on the latter parameters differs for low to moderate and high viscosity, displaying a transition at intermediate viscosity.

6. Trends in the mean size data coincide with those in the size distribution data. This suggests that knowledge of the breakup mechanism is required to properly interpret the results. Observations of breakage to date for low and moderate viscosity dispersed phases are consistent with a broadening of the distribution as μ_d increases. The transitions that occur at intermediate viscosity and differing functional dependencies at high viscosity may be due to a shift in the breakage mode as the total resistance to deformation increases.

The data demonstrate that dispersed-phase viscosity has a profound influence on both mean drop size and drop size distribution. However, they were obtained at constant interfacial tension. Viscosity and interfacial tension must be varied systematically in order to understand their relative importance and to yield correlations of practical significance. Such a study has been conducted for low to moderate viscosity dispersed phases and is reported in Part II of this paper.

Introduction

The prediction of heat and mass transfer and reaction rates in agitated liquid-liquid systems requires knowledge of the interfacial area. When two immiscible liquids are contacted, a dispersion is formed in which continuous breakup and coalescence of drops occur simultaneously. Eventually a local dynamic equilibrium is established for which the average drop size and size distribution depend on physical properties and conditions of agitation. This work focuses upon the extent to which physical properties, particularly dispersed-phase viscosity, affect the breakup process and the resulting equilibrium drop size. Therefore, discussion is limited to dilute suspensions for which coalescence is negligible. However, the results may apply to more concentrated dispersions when coalescence is minimized by the presence of stabilizing agents (Valentas et al., 1966). In a turbulent stirred tank contactor, drop breakup is believed to be confined to the impeller region, and is due to variations in turbulent pressure along the drop's surface (Hinze, 1955) and to stretch-

ing of globules in the trailing vortex system created by the impeller (Ali et al., 1981; Chang et al., 1981).

Consider a globule contained within an immiscible, turbulent continuous phase. The force associated with the continuous-phase turbulence works to distort the globule's surface and to break it into smaller drops. This force is balanced by the surface force due to interfacial tension and the force associated with the viscosity of the drop. If the dispersed-phase viscous force is large compared with the interfacial force, drop stability will be governed by the drop's viscosity. If the viscous force is small compared to the surface force, drop stability will be controlled by the latter. If these forces are of the same order, both will contribute to drop stability. An equilibrium drop size distribution will result when the disruptive force acting to split the globule is balanced by the cohesive forces acting to stabilize it.

Although turbulence-induced drop breakup in liquid-liquid contacting operations has commanded much attention, theory and experiments have mostly been limited to systems for which

the surface force is the dominant cohesive force. The work of many researchers, among them Shinnar and Church (1960) and Chen and Middleman (1967), has led to the development and verification of the well-known Weber number theory for prediction of the average equilibrium drop size. The semiempirical correlation that results is based on the local isotropy concept of Kolmogrov (1941a,b,c, 1949). As applied to dilute suspensions in baffled cylindrical tanks, the correlation is

$$\frac{D_{32}}{L} = A \ We^{-3/5} \quad (E_s \gg E_v) \tag{1}$$

$$We = \rho_c \ N^2 L^3 / \sigma \tag{2}$$

A is an experimentally determined constant which depends on tank geometry and impeller type. McManamey (1979) has attempted to correlate A with system geometry. An expression similar to Eq. 1 has been developed for static mixers by Middleman (1974). When Eq. 1 applies, the resulting drop size distributions have been shown to be normally distributed in volume both experimentally by Chen and Middleman (1967) and theoretically by Narsimhan et al. (1979).

The mechanistic arguments leading to Eq. 1 have been extended to account for dispersed-phase volume fraction and to develop population balance and Monte Carlo techniques to predict the evolution of the drop size distribution. An excellent review is given by Tavlarides and Stamatoudis (1981).

Several operations exist in which a viscous liquid is dispersed into turbulent continuous phase. Hinze (1955) established a basis for data correlation when both surface and dispersed-phase viscous forces contribute to drop stability. He proposed that two independent dimensionless groups were required and chose them to be a generalized Weber group, N_{We}, and a viscosity group, N'_{Vi}, both based on drop diameter.

$$N_{We} = \tau_c \ D/\sigma; \quad N'_{Vi} = \frac{\mu_d}{\sqrt{\rho_d \sigma D}} \tag{3}$$

Hinze further postulated that a drop would burst at a critical Weber number, which increases as the magnitude of N'_{Vi} increases, such that

$$(N_{We})_{crit} = C_1[1 + \psi(N'_{Vi})] \tag{4}$$

The function $\psi(N'_{Vi})$ decreases to zero for vanishing μ_d so that C_1 represents the critical Weber number for inviscid drops. Sleicher (1962) and Arai et al. (1977) applied Hinze's approach but had to redefine N'_{Vi} in order to correlate their limited data for pipes and stirred tanks, respectively.

Drop Size Correlations

Consider a dilute, turbulent liquid-liquid suspension. It is assumed that dispersed-phase globules are far apart and their presence does not influence the continuous phase except on scales of order of the globule size. The continuous-phase turbulent energy, which would be dissipated in a volume occupied by a globule, is instead transferred to it and acts to increase the globule's surface area and to overcome internal viscous resistance to flow. We look upon the globule as having cohesive energy composed of surface and viscous energy. Therefore, a

drop of size D is opposed by disruptive energy, E_T, due to continuous-phase turbulence, and is stabilized by cohesive energy due to interfacial tension, E_s, and dispersed-phase viscosity, E_v.

The disruptive energy is of order

$$E_T = \frac{1}{6}\Pi \ D^3 \ \tau_c \tag{5}$$

where τ_c is the turbulent energy per unit volume or the force per unit area acting on the drop. The surface energy is of order

$$E_s = \Pi \ D^2 \ \sigma \tag{6}$$

and the viscous energy is of order

$$E_v = \frac{1}{6}\Pi \ D^3 \ \tau_d \tag{7}$$

τ_d is a viscous energy per volume or a viscous stress within the drop.

The continuous phase may be described by an energy spectrum function, $E(k)$, such that $E(k) \ dk$ is the turbulent energy per unit mass associated with fluctuations of wave number k to $k + dk$. Therefore, τ_c is given by

$$\tau_c = \rho_c \int_{1/D}^{\infty} E(k)dk \tag{8}$$

Only energy associated with fluctuations of a scale smaller than $k = 1/D$ is considered since larger eddies convect the drop instead of deforming it. Shinnar (1961) argued that in turbulent stirred tank contactors, the maximum stable drop size is large compared to the microscale of turbulence but small compared with the macroscale. Therefore Kolmogorov's theory for the inertial subrange applies and $E(k)$ is given by

$$E(k) = \beta \ \epsilon^{2/3} \ k^{-5/3} \tag{9}$$

It is further assumed that the local and average energy dissipation rates per unit mass in the impeller region are related by a geometric constant (Chen and Middleman, 1967); that is,

$$\epsilon = C_2 \bar{\epsilon} \tag{10}$$

For baffled cylindrical tanks with $Re > 10^4$, Rushton et al. (1950) have shown that

$$\bar{\epsilon} = C_3 \ N^3 \ L^2 \tag{11}$$

According to Hinze (1955), continuous-phase turbulent fluctuations will cause flow velocities within the drop of order $\sqrt{\tau_c/\rho_d}$. Therefore, τ_d is of order

$$\tau_d = C_4 \ \mu_d \ \sqrt{\tau_c/\rho_d}/D \tag{12}$$

The maximum stable drop size results when the disruptive energy is equal to the cohesive energy. This state of dynamic equilibrium can be approximated by

$$E_T = E_s + E_v \quad (D = D_{max}) \tag{13}$$

Equation 13 is the basis for the correlation developed by Hughmark (1971) for turbulent pipe flow.

Equations 5–10, 12, and 13 can be combined for $D = D_{max}$ to yield

$$\frac{\rho_c \, \bar{\epsilon}^{2/3} D_{max}^{5/3}}{\sigma} = C_5 \left[1 + C_6 \left(\frac{\rho_c}{\rho_d} \right)^{1/2} \frac{\mu_d \, \bar{\epsilon}^{1/3} D_{max}^{1/3}}{\sigma} \right] \qquad (14)$$

In the limit as interfacial tension provides the dominant cohesive force, Eq. 14 reduces to

$$D_{max} = C_7 \frac{\sigma^{3/5}}{\rho_c^{3/5} \bar{\epsilon}^{2/5}} \quad (E_s \gg E_v) \qquad (15)$$

In the limit as dispersed-phase viscosity provides the dominant cohesive force, Eq. 14 reduces to

$$D_{max} = C_8 (\rho_c \, \rho_d)^{-3/8} \mu_d^{3/4} \bar{\epsilon}^{-1/4} \quad (E_v \gg E_s) \qquad (16)$$

Combining Eqs. 11 and 15 and comparing the result with Eq. 1 yields for $E_s \gg E_v$

$$D_{32} = C_9 D_{max} \qquad (17)$$

This result has been confirmed experimentally for inviscid dispersed phases by Brown and Pitt (1972).

Chen and Middleman (1967) derived Eq. 1 by proposing that the probability density function, $P(D)$, which describes the equilibrium drop size distribution, is only a function of E_T/E_s. If it is assumed that $P(D)$ is only a function of E_T/E_v, the method of Chen and Middleman can be applied, using Eqs. 5, 7–10, and 12 to obtain an expression for D_{32} that, when compared to Eq. 16, demonstrates the validity of Eq. 17 for very viscous drops. If Eq. 17 also applies when both E_s and E_v are finite, then Eqs. 11, 14, 15, and 17 can be combined to yield

$$\frac{D_{32}}{D_o} = [1 + B \, N_{Vi}]^{3/5} \qquad (18)$$

$$N_{Vi} = (\rho_c/\rho_d)^{1/2} \mu_d \, \bar{\epsilon}^{1/3} D_{32}^{1/3}/\sigma \qquad (19)$$

D_o is the Sauter mean diameter for inviscid dispersed phases as given by Eq. 1. The viscosity group, N_{Vi}, is the ratio of dispersed-phase viscous energy to surface energy. The limits $E_s \gg E_v$ and $E_v \gg E_s$ correspond to $N_{Vi} \rightarrow 0$ and $N_{Vi} \rightarrow \infty$, respectively. Eqs. 3, 8–10, 17, and 19 can be used to show that Eqs. 4 and 18 can be made identical by replacing N'_{Vi} by N_{Vi} and specifying $\psi(N_{Vi}) = B \, N_{Vi}$.

In the limit $N_{Vi} \rightarrow \infty$, Eqs. 1, 11, and 18 yield

$$\frac{D_{32}}{L} = C_{10} \left(\frac{\rho_c}{\rho_d} \right)^{3/8} \left(\frac{\mu_d}{\mu_c} \right)^{3/4} Re^{-3/4} \quad (E_v \gg E_s) \qquad (20)$$

$$Re = \rho_c \, N \, L^2/\mu_c \qquad (21)$$

Equation 20 is a convenient but somewhat misleading dimensionless form. Since μ_c is contained within Re, there is actually no dependency on μ_c, as should be the case.

Experiments and Data Reduction

In order to isolate the contribution of dispersed-phase viscosity, five silicone oils were dispersed in distilled water. These oils have a density close to water and exhibit constant interfacial tension with water, regardless of viscosity grade. Fluid physical properties are given in Table 1. Each oil is assigned a nominal viscosity to facilitate discussion. Densities were measured with a Westphal balance and interfacial tensions via an automated du Noüy ring method (Fisher Autotensiomat). Viscosities were measured with Cannon-Fenske viscometers. For the two most viscous oils, tests were conducted with a Rheometrics, Inc. mechanical spectrometer to determine if they exhibited shear-dependent viscosity. No change in viscosity was detected at shear rates up to 100 s^{-1}, and measured values agreed within 0.2% with those obtained with the Cannon-Fenske viscometers.

Experiments were conducted in four cylindrical, flat-bottom glass tanks of standard geometry using a photographic technique. A schematic diagram of the apparatus, including all geometric ratios, is given in Figure 1. Tank and impeller dimensions are given in Table 2. Each tank is assigned a nominal diameter to facilitate discussion. The impellers were driven by a variable speed Electro-Craft motor (model E-680 MGHR-5). The square, water-filled Plexiglas box that surrounds the tank served as a constant-temperature bath (maintained at 25°C) and allowed photographs to be taken through the cylindrical tank walls without optical distortion.

Preliminary experiments revealed that the higher viscosity silicone oils adhered readily to system surfaces. The problem was remedied by polishing metal surfaces to a mirror finish, employing an analytical grade cleaning procedure, and using ultrapure water as the continuous phase. Additionally, dead zones had to be eliminated by employing a large impeller to tank diameter ratio and by displacing the baffles a small distance from the bottom and sides of the tank. Arai et al. (1977) eliminated such surface sticking by adding a small amount of polyvinyl alcohol to the continuous phase (water).

The photographic system consisted of a Nikon F2A Photomic, 35mm SLR camera equipped with a 135 mm Nikor f:2.8 lens and a Nikon PB-4 bellows. The camera was focused on the impeller shaft (to determine magnification) with the bellows fully extended. The bellows-telephoto lens combination insured high magnification, shallow depth of field, due to the large lens-to-film distance, and negligible parallax error. Illumination was provided by a Sunpak Auto 611 thyristor-circuit electronic flash unit. The manually set flash duration of 0.00003 s (at 1/64

Table 1. Fluid Physical Properties at 25°C

Dispersed Phase, Silicone Oils*				
Nominal Viscosity μ'_d, Pa · s	Actual Viscosity μ_d, Pa · s	Density ρ_d, kg/m^3	Interfacial Tension** σ, N/m	No. Experiments Performed
0.1	0.0960	960	0.0378	32
0.5	0.486	971	0.0378	28
1	0.971	971	0.0378	36
5	4.43†	973	0.0378	14
10	10.51†	975	0.0378	16

Continuous Phase, Distilled Water
Viscosity, $\mu_c = 0.893 \times 10^{-3}$ Pa · s
Density, $\rho_c = 997$ kg/m^3

*Dow Corning 200 Fluids (dimethyl polysiloxane).
**With continuous phase.
†Average of values measured in Cannon-Fenske viscometer and Rheometrics mechanical spectrometer.
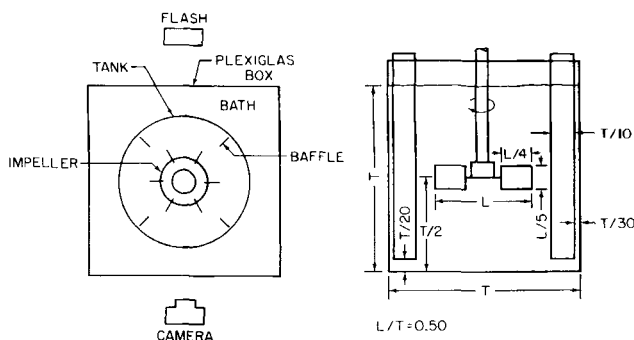
Figure 1. Schematic diagram of apparatus.

full power) was sufficiently fast to freeze droplet motion, since the sampling location was above the impeller region. Data were recorded on Kodak high contrast copy film.

With the impeller rotating in pure water at the selected speed, silicone oil was introduced via a syringe equipped with a large-diameter needle. The barrel of the syringe was depressed slowly so that globules much larger than the maximum stable drop size were introduced. The dispersed phase volume fraction was limited to $\phi \leq 0.0015$ to insure that a dilute noncoalescing suspension resulted. For dilute dispersions, the equilibrium drop size distribution is independent of spatial location (Chen and Middleman, 1967).

Preliminary experiments indicated that equilibrium was achieved in less than 1 h even for the highest viscosity oils. This is consistent with the data of Arai et al. (1977) for viscous dispersed phases. Therefore, after introducing them, a minimum of 1 h for the lower viscosity oils and 2 h for the higher viscosity oils was allowed before photographing the suspension.

Drop sizes were measured directly from the negatives by projecting them onto a screen with a 35 mm filmstrip projector. Grids located on the screen allowed drops to be classified into size groups at 50 μm intervals or greater. Mean drop size and size distribution were determined from 300 to 700 counts of drop diameter. The number of counts required to obtain a meaningful representation of the actual size distribution increased with dispersed-phase viscosity, as discussed later.

The Sauter mean diameter was calculated from

$$D_{32} = \sum_{i=1}^{M} n_i D_i^3 \bigg/ \sum_{i=1}^{M} n_i D_i^2 \qquad (22)$$

D_{32} is a convenient average, since interfacial area per unit volume is given by $a = 6\phi/D_{32}$. The functional form of the distribution can be examined by plotting cumulative frequencies on probability coordinates. The cumulative number frequency was

Table 2. Tank and Impeller Dimensions

Nominal Tank Dia. T' m	Actual Tank Dia. T m	Impeller Dia. L m	L/T
0.15	0.142	0.0711	0.50
0.2	0.213	0.1064	0.50
0.3	0.312	0.1562	0.50
0.4	0.391	0.1956	0.50

calculated from

$$F_n(D_i) = \sum_{J=1}^{i} n_J \bigg/ \sum_{J=1}^{M} n_J \qquad (23)$$

A total of 126 experiments were performed at impeller speeds ranging from 0.93 to 5.95 rps. The higher speeds were limited to the smaller tanks, due to entrainment of air at the free surface in the larger tanks at higher N. The number of experiments performed with each oil is given in Table 1. The range of variables studied includes $13,000 < Re < 101,000$, $44 < We < 1,137$, and $0.065 < \bar{\epsilon} < 0.50$ m²/s³.

Drop Size Distribution Data

Typical number distributions at various dispersed-phase viscosities are given on normal probability coordinates in Figures 2 and 3. As μ_d increases, the distribution broadens considerably. The size of the largest drops increases while their number decreases, and the size of the smallest drops decreases while their number increases. For the 0.1 and 5 Pa · s oils of Figure 2, the percentage of drops smaller than 100 μm is 7 and 15%, respectively.

The moderate-viscosity (0.1 and 0.5 Pa · s) data are normally distributed in number. The number median and Sauter mean diameters differ by a relatively small amount, but this difference increases with μ_d. On the average, data for these oils were equally well represented by a normal distribution in volume. Size distributions for low and moderate dispersed-phase viscosities are discussed in detail in Part II of this paper.

For the high-viscosity (5 and 10 Pa · s) oils, the large-diameter tail of the distribution is extremely broad. There are numerous small drops and relatively few large drops. The number median and Sauter mean diameters differ substantially. The few largest drops determine D_{32}. For the data of Figure 3, 98.3 and 98.8% of the drops are smaller than D_{32} for the 5 and 10 Pa · s oils, respectively. The largest 1% of the drops contain over 70% of the dispersed-phase volume, so volume distribution data yield little useful information. The 5 Pa · s data of Figure 3 are
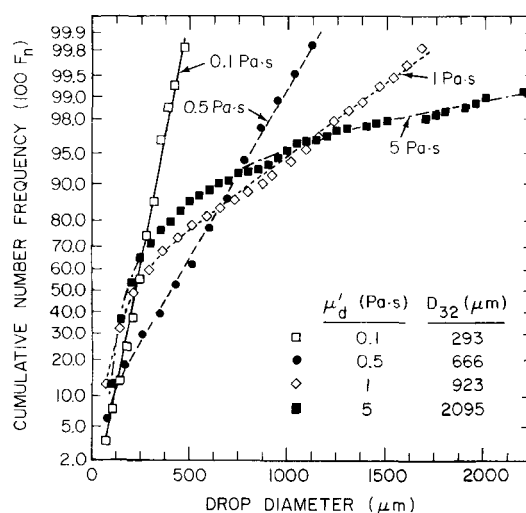

Figure 2. Effect of dispersed-phase viscosity on drop size distribution, normal probability coordinates. $T' = 0.3$ m; $N = 2.0$ rps.
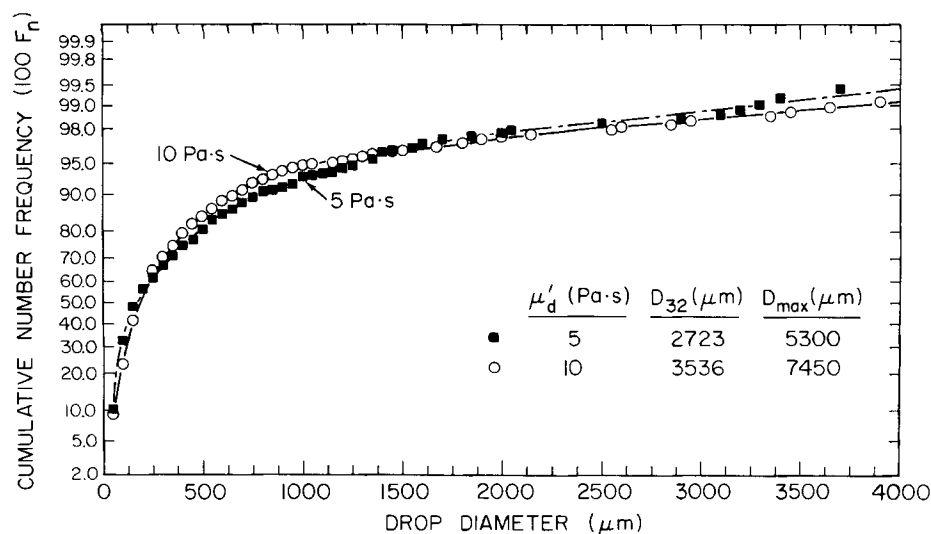
Figure 3. Similarity of drop size distributions for high-viscosity dispersed phases, normal probability coordinates. $T' = 0.2$ m; $N = 2.0$ rps.

replotted on log-normal probability coordinates in Figure 4, indicating that the high-viscosity data tend to be log-normally distributed in number.

Given the relatively few large drops at high viscosity, the assumption that equilibrium was achieved after 2 h of stirring was tested. A few experiments were run for long periods to insure that each drop experienced the entire impeller region volume. Several of the largest drops deformed but again became spherical. It was concluded that the largest drops were indeed stable because they do not remain in the impeller region long enough to break.

It was not possible to characterize the functional form of the distribution for the 1 Pa · s oil because it varied for different conditions of agitation. It can be concluded that for the range of variables studied, the functional form of the number distribution tends from normal to log-normal as μ_d increases. However, for

Figure 4. Drop size distribution for high-viscosity dispersed phase, log-normal probability coordinates. $\mu_d' = 5$ Pa · s; $T' = 0.2$ m; $N = 2.0$ rps.

different interfacial tension or higher power input, the functional form for a particular dispersed-phase viscosity may differ from the results of this study.

The effect of dispersed-phase viscosity on the size distribution is not unique to viscous dispersed phases. Noro (1978) and Karabelas (1978) studied drop breakup in stirred tanks and pipes, respectively, for viscosity ratios (μ_d/μ_c) less than unity. Noro found that as the viscosity ratio decreased, the size distribution broadened. Both found that drop sizes were log-normally distributed at lower viscosity ratios.

Mean Drop Size Data

Given the effect of μ_d on the drop size distribution, mean values of D_{32}/D_{max} were calculated for each grade of oil. These and the average value for all runs are given in Table 3. The average value for the inviscid, dilute dispersed-phase data of Chen and Middleman (1967), who employed the geometry of Figure 1, is also given. This was calculated from the raw data reported by Chen (1966). For the moderate-viscosity oils $D_{32} \simeq 0.6\ D_{max}$, which is within one standard deviation of the inviscid result. For the high-viscosity oils $D_{32} \simeq 0.5\ D_{max}$, an interesting result given is that D_{32} is determined by the few largest drops. Analysis of the data for these oils indicates that D_{32} is actually a better measure
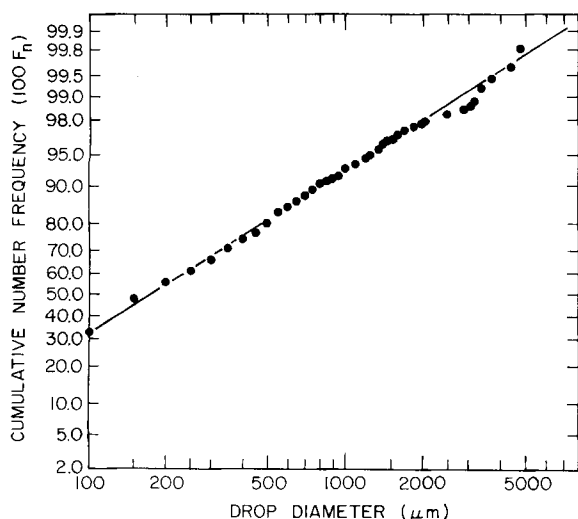
Table 3. Relationship Between D_{32} and D_{max}

Nominal Dispersed-Phase Viscosity μ_d', Pa · s	Mean D_{32}/D_{max}	Standard Deviation	% Std. Dev.*
0.1	0.59	0.082	13.8
0.5	0.60	0.098	16.4
1	0.56	0.081	14.1
5	0.48	0.053	11.1
10	0.52	0.055	10.6
Average	0.56	0.080	14.2
Chen and Middleman (1967) (110 data sets)	0.64	0.053	8.3

*% Std. Dev. = 100 × Std. Dev. ÷ Mean D_{32}/D_{max}.

of the largest drops than D_{max} since correlations show less scatter when based on the former. On the average, D_{32}/D_{max} decreases as μ_d increases. However, all mean values and the inviscid average fall within one standard deviation of the overall average for this study. Therefore, Eq. 17 is approximately valid for both inviscid and viscous dispersed phases.

If Eq. 18 is valid, then a plot of $Z^{5/3} = (D_{32}/D_o)^{5/3}$ vs. N_{Vi} should yield a straight line of slope B. To develop this plot, D_o was estimated from Eq. 1 with $A = 0.053$ (Chen and Middleman, 1967) and $\bar{\epsilon}$ was estimated from Eq. 11 with $C_3 = 0.97$ (Rushton et al., 1950). The results are presented in Figure 5. The uniform dashed lines of the insert and main plot are the same. The shaded area of the insert represents the region containing all the 0.1 Pa · s data. The data of Arai et al. (1977) are also given. These authors used the geometry of Figure 1 to disperse polystyrene-o-xylene solutions in water. They reported the ratio of maximum stable drop size to that in the absence of viscosity. Given Eq. 17, this ratio is equivalent to Z. The limited data of Arai et al. show similar trends to the data of this study. They achieved higher values of N_{Vi}, for a given μ_d, than here due to lower interfacial tension and higher impeller speeds.

For the moderate-viscosity oils, Eq. 18 appears to be valid although there is scatter in the 0.5 Pa · s data, indicating a dependency on tank size. These data are approximated by

$$\frac{D_{32}}{D_o} = [1 + 11.5 \, N_{Vi}]^{5/3} \quad (N_{Vi} < 1) \qquad (24)$$

The 1 Pa · s data show considerable scatter. N_{Vi} does not appear to be a relevant parameter and it seems that no model based on power per unit mass ($\bar{\epsilon}$) will provide a reasonable correlation.

The high-viscosity data show a linear dependency on N_{Vi} but of slope less than that for moderate viscosity. N_{Vi} appears to be a relevant correlating parameter even though Eq. 18 does not apply. Equation 18 could be made to coincide with these data if A in Eq. 1 were replaced by an arbitrary constant of larger magnitude.

It is interesting to note that the linear region in Figure 5 for moderate viscosity coincides with number distributions that are normally distributed, while the linear region of lesser slope at high viscosity coincides with log-normal size distributions. The "transition" region of large scatter coincides with size distributions that cannot be characterized. On the average, $Z^{5/3}$ may be approximated by a power law function of N_{Vi}; that is, $\psi(N_{Vi}) = B \, N_{Vi}^{C_{11}}$ where $C_{11} < 1$ (see discussion following Eq. 19).

Since $Z^{5/3}$ depends linearly on N_{Vi} at high dispersed-phase viscosity, Eq. 20 may still apply at large N_{Vi}, although C_{10} will not be related to the constants in Eq. 24. Figure 6 gives D_{32}/L vs. Re for each viscosity grade. Best-fit lines were determined via nonlinear least-squares regression. Inviscid data obtained by Chen and Middleman (1967) for dilute chlorobenzene dispersions in water are shown for comparison. This system has the same interfacial tension as silicone oil-water.

The data correlate well with Re in that each viscosity grade displays a distinct best-fit line. The scatter is largest for the 1 Pa · s oil as expected. No systematic dependency on tank size is seen. As μ_d increases slopes decrease until the high-viscosity limit is reached. There is then an abrupt change in slope to a higher constant value of $s \simeq -3/4$. This is the Reynolds number dependency predicted by Eq. 20, indicating that the limit of negligible surface force has been reached. However, this is not the case. The high-viscosity data are well correlated (since $\rho_c =$
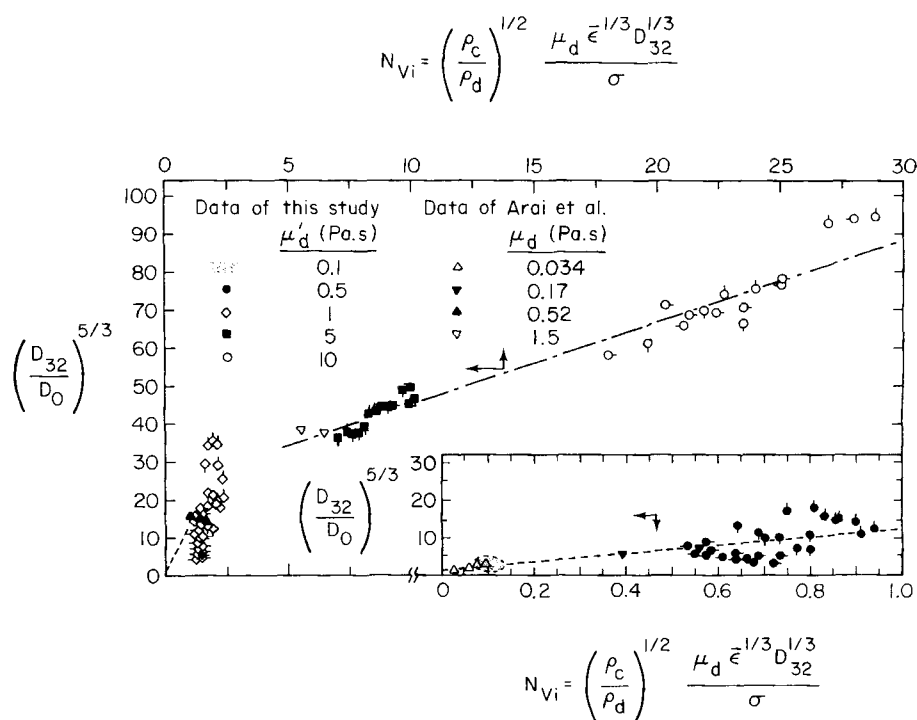
$$N_{Vi} = \left(\frac{\rho_c}{\rho_d}\right)^{1/2} \frac{\mu_d \, \bar{\epsilon}^{1/3} D_{32}^{1/3}}{\sigma}$$

Figure 5. Dependency of Sauter mean diameter on viscosity group.

For data of this study, tick marks on symbols indicate tank size. Tick: above, $T' = 0.15$ m; below, $T' = 0.2$ m; right, $T' = 0.3$ m; left, $T' = 0.4$ m.
For data of Arai et al. (1977): $\sigma = 0.022$ N/m; $T = 0.127$ m; $2.5 \leq N \leq 13.6$ rps; $\phi \leq 0.003$.
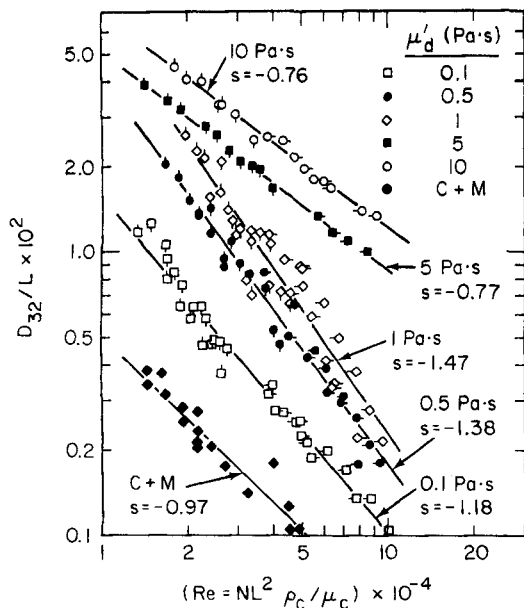
Figure 6. Dimensionless Sauter mean diameter vs. tank Reynolds number.

For data of this study tick marks on symbols indicate tank size as in Fig. 5. C + M: data of Chen and Middleman (1967) for chloro-benze dispersions in water with $\sigma = 0.0377$ N/m; $\mu_d = 0.00078$ Pa · s; $0.051 \le L \le 0.152$ m; $1.5 \le N \le 8.3$ rps; $0.001 < \phi < 0.005$.

ρ_d) by

$$\frac{D_{32}}{L} = 2.1 \left(\frac{\mu_d}{\mu_c}\right)^{3/8} Re^{-3/4} \qquad (25)$$

The goodness of fit is shown in Figure 7. The dependency on dispersed-phase viscosity is half that predicted by the semiempirical theory. This may be due to high interfacial tension. At these high viscosities the σ contribution should be relatively small and may manifest itself as an effective viscosity. From Eqs. 11 and 20 it is evident that if $D_{32}/L \sim Re^{-3/4}$ then $D_{32} \sim \bar{\epsilon}^{-1/4}$. The high-viscosity data are equally well fit by a correlation of the form $D_{32} \sim \mu_d^{3/8} \bar{\epsilon}^{-1/4}$. Equation 25 is a convenient dimensionless form.
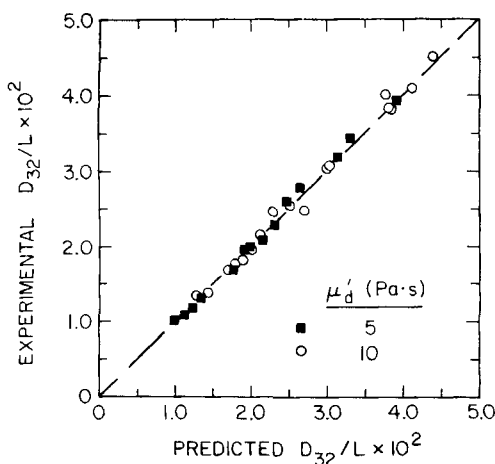

Figure 7. Goodness of fit of Eq. 25 to high-viscosity data.

However, μ_c is constant here, and extension to other liquids (of equal σ) is best accomplished in terms of μ_d and $\bar{\epsilon}$.

Practitioners are aware that in some cases mean drop size data correlate well with power per unit mass ($\bar{\epsilon}$) and in other cases with tip speed ($=\Pi NL$). A correlation with tip speed is given in Figure 8, with μ_d as a parameter. The correlation is reasonably good, showing no systematic dependency on tank size; the slopes of the curves show similar trends to those of Figure 6.

Discussion

Consider the high-viscosity data with respect to Eq. 18 and Figure 5. The largest scales of turbulence are of order of the blade width. Therefore Eq. 9 may not be valid since $W/L = 0.2$ while $0.02 < D_{max}/L < 0.09$ (Figure 6 and Table 3). The functional form of $E(k)$ is such that for large drops, use of Eq. 9 in 8 will overestimate τ_c so that D_{32} will be underestimated by Eq. 18. D_{32} will also be underestimated if viscous drops do not remain in the impeller region long enough to break. These arguments suggest that B should increase with μ_d so, although reasonable, they cannot account for observed behavior.

The close relationship between trends in the mean size and size distribution data suggest that observations of drop breakage are required to properly interpret the results. Stephenson (1974) and Collins and Knudsen (1970) observed the breakage of small, low-viscosity drops in turbulent stirred tanks and pipes, respectively. These drops stretched to form dumbbell-like structures prior to breakage. Konno et al. (1983) observed that in the vicinity of Rushton turbines, these dumbbells fractured to form about three daughters. Ali et al. (1981) and Chang et al. (1981) studied the breakup of large, moderate-viscosity oil globules in water behind large impellers of several geometries. They observed a spectrum of breakage modes ranging from bursting to
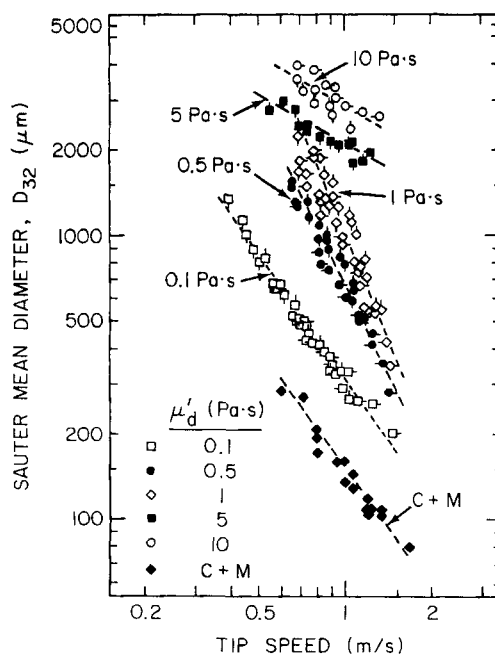

Figure 8. Correlation with tip speed.

For data of this study tick marks on symbols indicate tank size as in Fig. 5. The data of Chen and Middleman, 1967 (C + M) are as in Fig. 6.

stretching. Turbulent bursting occurred at high Reynolds number and resulted in numerous daughter drops of relatively narrow size distribution. Ligament stretching occurred at lower Reynolds numbers and was characterized by a broader distribution of daughter sizes. As drop viscosity increased, breakage shifted from bursting toward stretching.

Equations 5–9 and 12 can be manipulated to show that the resistance to breakage, $(E_s + E_v)/E_T$, increases as μ_d and σ increase and as D and ϵ decrease. Therefore, observations to date indicate a transition from bursting to stretching as the resistance to breakage increases, and are consistent with a broadening of the distribution as μ_d increases. It is difficult to interpret the results for $\mu_d' \geq 1$ Pa · s since no observations of breakage exist. The presence of numerous small drops suggests that the disintegration process may be somewhat different. An extreme form of stretching may predominate by which the fracture of highly elongated dumbbells produces satellite droplets. Alternatively, breakage may only occur close to impeller surfaces and may therefore be more erosive (stripping of small daughters from the parent) as defined by Narsimhan et al. (1980). If deformation modes differ at moderate and high viscosity, then C_4 in Eq. 12 and therefore B in Eq. 18 may also differ. A transition region could exist that shifts to higher viscosity as interfacial tension decreases. Such may also be the case at high power input. A third parameter, perhaps one that represents the total resistance to breakage, may be required to define the transition. More definitive statements must await systematic observations of breakup for a wide range of parameters.

A final concern is the rheological behavior of viscous silicone oils. Certain grades are known to be weakly elastic although they do not exhibit shear-dependent viscosity (Kelkar et al., 1972). However, Boger (1980) points out that these fluids are sold commercially as Newtonian standards and have been used to investigate viscous Newtonian behavior. Weinberger and Goddard (1974) measured the extensional viscosity of a 100 Pa · s silicone oil in constant force spinning and found it to be Newtonian for $0.6 < \dot{\gamma}_e < 10$ s^{-1}. Weinberger and Donnelly (1975) found that fiber-spinning data for this oil were well fit by a Newtonian model at extension rates (estimated from their data) up to $\dot{\gamma}_e = 31.1$ s^{-1}. McClelland and Finlayson (1983) found that squeezing flows for a 106 Pa · s silicone oil were well-predicted by a Newtonian model. Boger (1980) measured material parameters for silicone oils in steady, simple shear flow (SSF). A 13.3 Pa · s oil exhibited second-order behavior with $S_R = \lambda \dot{\gamma}_s = 0.00088 \dot{\gamma}_s$ for $20 < \dot{\gamma}_s < 200$ s^{-1}.

A conservative estimate of the maximum strain rate within a drop can be obtained as follows. Assume that $\tau_c = \mu_d \dot{\gamma}_D$ and recall that Eq. 8 with Eq. 9 overestimates τ_c for large drops. The Kolmogorov constant is $\beta = 1.5$ (Tennekes and Lumley, 1972). Several workers, among them Cutter (1966), Rao and Brodkey (1972), van der Molen and van Maanen (1978), and Bertrand et al. (1980), have measured turbulence parameters and/or the spatial variation of local energy dissipation rate within the impeller stream. Estimates of ϵ_{max} vary widely depending upon the technique employed. Most significant are the studies of Nishikawa et al. (1976) and Okamoto et al. (1981). These authors obtained accurate estimates of ϵ by achieving unambiguous measurements of the high-frequency components of the energy spectrum via hot film anenometry. They found that for Rushton turbines, ϵ_{max} was sensitive to L/T. For the geometry of this study, $\epsilon_{max} \simeq 8\bar{\epsilon}$. Employing this estimate with Eqs. 8 and 9

yields

$$\dot{\gamma}_D \simeq 9 \, \rho_c \, \bar{\epsilon}^{2/3} \, D^{2/3}/\mu_d \tag{26}$$

Consider a drop that is five times larger than D_{max}. For the 10 Pa · s oil ($D_{max} = 0.52 \, D_{32}$; $4,000 > D_{32} > 2,350 \, \mu$m for $0.065 < \bar{\epsilon} < 0.5$ m^2/s^3), Eq. 26 yields $16 < \dot{\gamma}_D < 43$ s^{-1}.

These strain rates are in the range for which the cited studies with spatially varying kinematics (spinning and squeezing) indicate Newtonian behavior for a silicone oil that is ten times more viscous. The Boger data for a 13.3 Pa · s oil in steady SSF yield $0.014 < S_R < 0.038$ in this range. The recoverable shear, a form of Weissenberg number for a second-order fluid, is a measure of elastic to viscous effects (Middleman, 1977). A measure of transient effects can be obtained by estimating the Deborah number, $De = \lambda/\theta_D$, based on the Boger data and a characteristic time of deformation, θ_D, for a drop in the impeller region. The high-speed cine data of Ali et al. (1981) and Chang et al. (1981) indicate that the characteristic time for deformation and breakup of a large globule ($\mu_d \sim 0.2$ Pa · s; $N \sim 1.5$ rps) undergoing ligament stretching is of order $\theta_D \geq 0.1$ s. A smaller, more viscous drop is expected to deform more slowly, so this estimate should be a reasonable upper bound for the 10 Pa · s data of this study. Using $\lambda = 0.00088$ s (Boger, 13.3 Pa · s oil), $De \leq 0.01$, indicating that the viscosity is steady with respect to the time scale of deformation. It appears, to a first approximation, that elastic effects are unimportant for the 10 Pa · s data of this study. It is unlikely that the lower viscosity oils would be more elastic. However, these arguments are by no means definitive, since the kinematics of a deforming drop differs from the aforementioned flows.

Acknowledgment

Notation

A = dimensionless empirical constant, Eq. 1
a = interfacial area per unit volume
B = dimensionless empirical constant, Eq. 18
$C_1 \ldots C_{11}$ = dimensionless empirical constants
D = diameter of drop
$De = \lambda/\theta_D$ = Deborah number
D_i = drop diameter representing the ith size interval
D_{max} = maximum stable drop diameter
D_o = Sauter mean diameter of an inviscid drop, Eq. 1
D_{32} = Sauter mean diameter
$E(k)$ = energy spectrum function
E_s = surface energy of drop
E_T = turbulent energy available to disrupt drop
E_v = viscous energy of drop
F_n = cumulative number frequency
k = wave number
L = impeller diameter
M = number of drop size intervals
N = impeller speed
N_{Vi} = viscosity group, Eq. 19
N'_{Vi} = viscosity group, Eq. 3b
N_{We} = generalized Weber group, Eq. 3a
n_i = number of drops in the ith size interval

$P(D)$ = probability density function for equilibrium drop size distribution

Re = tank Reynolds number, Eq. 21

$S_R = (\tau_{11} - \tau_{22})/(2\tau_{12})$ = recoverable shear

s = slope of line

T = tank diameter

T' = nominal tank diameter

W = width of impeller blade

We = tank Weber number, Eq. 2

$Z = D_{32}/D_o$ = ratio of Sauter mean diameter of a viscous drop to that of an inviscid drop

Greek letters

β = Kolmogorov constant, Eq. 9

$\dot{\gamma}_D$ = maximum strain rate within drop

$\dot{\gamma}_e$ = extension rate in elongational flow

$\dot{\gamma}_s$ = shear rate in steady, simple shear flow

ϵ = local energy dissipation rate per unit mass

$\bar{\epsilon}$ = average power input per unit mass or mean energy dissipation rate per unit mass

ϵ_{max} = maximum energy dissipation rate per unit mass in impeller region

λ = elastic relaxation time

θ_D = characteristic time scale for deformation and breakup of a drop

μ_c = viscosity of continuous phase

μ_d = viscosity of dispersed phase

μ'_d = nominal dispersed-phase viscosity

ρ_c = density of continuous phase

ρ_d = density of dispersed phase

σ = interfacial tension

τ_c = turbulent energy per unit volume or force per unit area acting on drop

τ_d = dispersed-phase viscous energy per unit volume or viscous stress within drop

$\tau_{11} - \tau_{22}$ = primary normal stress difference

τ_{12} = shear stress

ϕ = volume fraction of dispersed phase

$\psi(x)$ = unknown function of x

Literature Cited

Ali, A. M., et al., "Liquid Dispersion Mechanisms in Agitated Tanks. I: Pitched-Blade Turbine," *Chem. Eng. Commun.*, 10, 205 (1981).

Arai, K., et al., "The Effect of Dispersed-Phase Viscosity on the Maximum Stable Drop Size for Breakup in Turbulent Flow," *J. Chem. Eng. Japan*, 10, 325 (1977).

Bertrand, J., J. P. Couderc, and H. Angelino, "Power Consumption, Pumping Capacity, and Turbulence Intensity in Baffled Stirred Tanks: Comparison Between Several Turbines," *Chem. Eng. Sci.*, 35, 2,157 (1980).

Boger, D., "Separation of Shear Thinning and Elastic Effects in Experimental Rheology," in *Rheology, 1, Principles*, G. Astarita, G. Marrucci, and L. Nicolais, Ed., Plenum, New York, 195 (1980).

Brown, D. E., and K. Pitt, "Drop Size Distribution of Stirred Noncoalescing Liquid-Liquid System," *Chem. Eng. Sci.*, 27, 577 (1972).

Chang, T. P. K., et al., "Liquid Dispersion Mechanisms in Agitated Tanks. II: Straight-Blade and Disc Style Turbines," *Chem. Eng. Commun.*, 10, 215 (1981).

Chen, H. T., "Drop Size Distribution in Agitated Tanks," Ph.D. Thesis, Univ. of Rochester, NY (1966).

Chen, H. T., and S. Middleman, "Drop Size Distribution in Agitated Liquid-Liquid Systems," *AIChE J.*, 13, 989 (1967).

Collins, S. B., and J. G. Knudsen, "Drop Size Distributions Produced by Turbulent Pipe Flow of Immiscible Liquids," *AIChE J.*, 16, 1,072 (1970).

Cutter, L. A., "Flow and Turbulence in a Stirred Tank," *AIChE J.*, 12, 35 (1966).

Hinze, J. O., "Fundamentals of the Hydrodynamic Mechanism of Splitting in Dispersion Processes," *AIChE J.*, 1, 289 (1955).

Hughmark, G. A., "Drop Breakup in Turbulent Pipe Flow," *AIChE J.*, 17, 1,000 (1971).

Karabelas, A. J., "Droplet Size Spectra Generated in Turbulent Pipe Flow of Dilute Liquid-Liquid Dispersions," *AIChE J.*, 24, 170 (1978).

Kelkar, J. V., R. A. Mashelkar, and J. Ulbrecht, "On the Rotational Viscoelastic Flows around Simple Bodies and Agitators," *Trans. Inst. Chem. Engrs.*, 50, 343 (1972).

Kolmogorov, A. N.,. "The Local Structure of Turbulence in Incompressible Viscous Fluid for Very Large Reynolds Numbers," *Compt. Rend. Acad. Sci. USSR*, 30, 301 (1941a).

———, "On Degeneration of Isotropic Turbulence in an Incompressible Viscous Liquid," *Compt. Rend. Acad. Sci. USSR*, 31, 538 (1941b).

———, "Dissipation of Energy in Locally Isotropic Turbulence," *Compt. Rend. Acad. Sci. USSR*, 32, 16 (1941c).

———, "The Breakup of Droplets in a Turbulent Stream," *Dok. Akad. Nauk.*, 66, 825 (1949).

Konno, M., M. Aoki, and S. Saito, "Scale Effect on Breakup Process in Liquid-Liquid Agitated Tanks," *J. Chem. Eng. Japan*, 16, 312 (1983).

McClelland, M. A., and B. A. Finlayson, "Squeezing Flow of Elastic Fluids," *J. Non-Newtonian Fluid Mech.*, 13, 181 (1983).

McManamey, W. J., "Sauter Mean and Maximum Drop Diameters of Liquid-Liquid Dispersions in Turbulent Agitated Vessels at Low Dispersed-Phase Hold-up," *Chem. Eng. Sci.*, 34, 432 (1979).

Middleman, S., "Drop Size Distributions Produced by Turbulent Pipe Flow of Immiscible Fluids through a Static Mixer," *Ind. Eng. Chem. Process Des. Dev.*, 13, 78 (1974).

Middleman, S., *Fundamentals of Polymer Processing*, McGraw-Hill, New York (1977).

Narsimhan, G., J. P. Gupta, and D. Ramkrishna, "A Model for Transitional Breakage Probability of Droplets in Agitated Lean Liquid-Liquid Dispersions," *Chem. Eng. Sci.*, 34, 257 (1979).

Narsimhan, G., D. Ramkrishna, and J. P. Gupta, "Analysis of Drop Size Distributions in Lean Liquid-Liquid Dispersions," *AIChE J.*, 26, 991 (1980).

Nishikawa, M., et al., "Turbulence Energy Spectra in Baffled Mixing Vessels," *J. Chem. Eng. Japan*, 9, 489 (1976).

Noro, S., "Studies on Liquid-Liquid Disperson by Mechanical Agitation," *Prog. Organic Coatings*, 6, 271 (1978).

Okamoto, Y., M. Nishikawa, and K. Hashimoto, "Energy Dissipation Rate Distribution in Mixing Vessels and Its Effects on Liquid-Liquid Dispersion and Solid-Liquid Mass Transfer," *Int. Chem. Eng.*, 21, 88 (1981).

Rao, M. A., and R. S. Brodkey, "Continuous-flow Stirred Tank Turbulence Parameters in the Impeller Stream," *Chem. Eng. Sci.*, 27, 137 (1972).

Rushton, J. H., E. W. Costich, and H. J. Everett, "Power Characteristics of Mixing Impellers," Part I, *Chem. Eng. Prog.*, 46, 395 (1950); Part II, *Chem. Eng. Prog.* 46, 467 (1950).

Shinnar, R., "On the Behavior of Liquid Dispersions in Mixing Vessels," *J. Fluid Mech.*, 10, 259 (1961).

Shinnar, R., and J. M. Church, "Predicting Particle Size in Agitated Dispersions," *Ind. Eng. Chem.*, 52, 253 (1960).

Sleicher, C. A., Jr., "Maximum Stable Drop Size in Turbulent Flow," *AIChE J.*, 8, 471 (1962).

Stephenson, R., "The Effect of Agitation on Stirred Suspension Drop Size: A Model Study," *Inst. Chem. Eng. Symp. Ser.* No. 38, C4.1–22 (1974).

Tavlarides, L. L., and M. Stamatoudis, "The Analysis of Interphase Reactions and Mass Transfer in Liquid-Liquid Dispersions," *Adv. Chem. Eng.*, 11, 199 (1981).

Tennekes, H., and J. L. Lumley, *A First Course in Turbulence*, MIT Press, Cambridge, MA (1972).

Valentas, K. J., O. Bilous, and N. R. Amundson, "Analysis of Breakage in Dispersed-Phase Systems," *Ind. Eng. Chem. Fund.*, 5, 271 (1966).

van der Molen, K., and H. R. E. van Maanen, "Laser Doppler Measurements of Turbulent Flow in Stirred Vessels to Establish Scaling Rules," *Chem. Eng. Sci.*, 33, 1,161 (1978).

Weinberger, C. B., and G. J. Donnelly, "Stability of Isothermal Fiber Spinning of a Newtonian Fluid," *Ind. Eng. Chem. Fund.*, 14, 334 (1975).

Weinberger, C. B., and J. D. Goddard, "Extensional Flow Behavior of Polymer Solutions and Particle Suspensions in a Spinning Motion," *Int. J. Multiphase Flow*, 1, 465 (1974).